UNIVERSITY OF ILLINOIS

May 1989

THIS IS TO CERTIFY THAT THE THESIS PREPARED UNDER MY SUPERVISION BY

AREJAS J. UZGIRIS

ENTITLED INTERNAL ENERGY OF METHANOL CLUSTERS IN SUPERSONIC MOLECULAR BEAMS

IS APPROVED BY ME AS FULFILLING THIS PART OF THE REQUIREMENTS FOR THE

DEGREE OF BACHELOR OF SCIENCE IN CHEMISTRY

James M. Lisy
Instructor in Charge

APPROVED: Thomas H. Hummel

for HEAD OF DEPARTMENT OF CHEMISTRY

O-1364

Internal Energy of Methanol Clusters in Supersonic Molecular Beams

By
Arejas J. Uzgiris

Thesis

for the
Degree of Bachelor of Science
in
Chemistry

College of Liberal Arts and Sciences
University of Illinois
Urbana, Illinois

1989

ACKNOWLEDGEMENTS

Many thanks to my parents for providing the oppurtunity and the motivation; to Professor James Lisy, my advisor, for the direction; and everyone in the group for the help and the company. The Jeffs deserve special thanks because they actually did all the work. Joe gets a mention since he participated in the crucial stress-relieving activities on the quad that made working in the lab sufferable on those beautiful spring days. Gail gets ultraspecial thanks because she kept my confidence up and brought some sunshine into each day even when the weather forecast was dismal. To one and all, thanks for the good times.

TABLE OF CONTENTS

INTRODUCTION

This is an investigation of the internal temperature of methanol clusters produced in a molecular beam. This research is directly related to the predissociation spectroscopy of these same species. A determination of the velocities of these clusters is needed for eventually calculating absolute values for their photodissociation cross-sections. Temperatures collected here represent a quantification of the cooling process in gas expansion beam formation.

Earlier studies on gases in free expansion jets were mostly concerned with the behavior of simple noninteracting beam molecules; any clustering was only considered as a source of experimental error. An example of this can be found in reference 1. In-depth analyses of supersonic nozzle beams are contained in references 2 and 3. The research presented here applies similar methods but treats the clusters as the main species of interest. This was done with water clusters in 1981 by Dreyfuss and Wachman[4], but due to the high background levels associated with the water vapor experiments we found the study of methanol clusters more rewarding.

EXPERIMENTAL

Two machines were used to collect the time-of-flight (TOF) data. The recently completed ion-beam machine in its neutral beam configuration is shown in figure 1. The original neutral beam apparatus is an earlier design with cluster formation and detection stages that differ significantly from the ion machine. Figure 2 shows the neutral beam apparatus with its off-axis detection system. Placing the detector perpendicular to the beam axis reduces the sensitivity with respect to large (>400 amu) clusters. Because of this complication the ion machine must be used to investigate heavier clusters.

The ion-beam apparatus is composed of two chambers. The source chamber is pumped by a HS-10 diffusion pump at 4000 Liters/Sec. The detector chamber uses a VHS-6 at 2200 Liters/Sec. Both are backed by mechanical pumps capable of 8.5 Liters/Sec pumping speed. At standard backing pressures for the inlet gas the source pressure remains less than 10^{-4} Torr and the detector chamber stays below 10^{-6} Torr.

Included in the setup are a series of electrostatic lenses that guide the ions toward the detector. In the neutral mode the source-lens system is bypassed, but the detector lenses and quadrupole remain in use. The quadrupole is an Extranuclear model 7-162-8 with a length of 21 cm.. A channel electron multiplier (CEM) is used for detecting electron pulses generated by the conversion dynode. The output of a multichannel scaler (MCS) is sent to a Digital PDP-

11/73 microcomputer. The files are later transferred to a Vax mainframe for analysis.

The equipment details included here were chosen because of their importance in the use of the ion-beam apparatus in its previously undocumented neutral beam configuration. Several other sources are available for more complete descriptions of the two beam machines in their laser dissociation configurations.[5,6,7]

The formation of the solvated ion beam is accomplished by passing the carrier gas containing the solvent (in this case 10% methanol in argon) past a hot filament coated with the desired metallic cation source. In neutral beam experiments a simpler setup suffices. Various rare gases can be used either by themselves or bubbled through a liquid solvent to create the desired beam composition. In this case argon was used as the carrier gas and was bubbled through liquid methanol. This gaseous mixture was then channeled through a nozzle and into the vacuum chamber. The expansion and subsequent skimming creates a narrow supersonic molecular beam. By experimenting with source conditions, the characteristics of the expansion can be tuned to adjust the cluster distribution.

The TOF apparatus was designed to be portable and usable by both of the machines in our lab; the wheel assembly attaches to a keyed flange on each source chamber. The chamber must be vented to the atmosphere before disassembly. Although repressurization only takes a little while if the diffusion pumps are closed off and left hot during the reconfiguration, the condensation of water vapor on the inner surfaces during the change takes at least several hours to

pump off. The TOF wheel must be carefully positioned and a routine check of the inner connections of all the accessible parts is undertaken. The use of HF in the neutral machine necessitates more frequent repair of various metal and synthetic parts. O-rings on both machines must be periodically replaced because of swelling caused by pump oil contamination. After closing the chamber and pumping down, the gas source must be adjusted to the proper settings and is allowed some time to reach a consistent composition.

Data is collected by a customized software package that includes plotting capability during data collection to keep track of noise bursts and other signal problems that can ruin data. After collection, the data files are transfered to a VAX mainframe, where they are reformatted for the TOF program. The program Kelvin[8] running on the departmental Vax processing cluster provided the computing power needed for converting trajectory data into velocity distributions, beam temperatures, and flow velocities.

Figure 1. Ion-beam apparatus in neutral configuration.

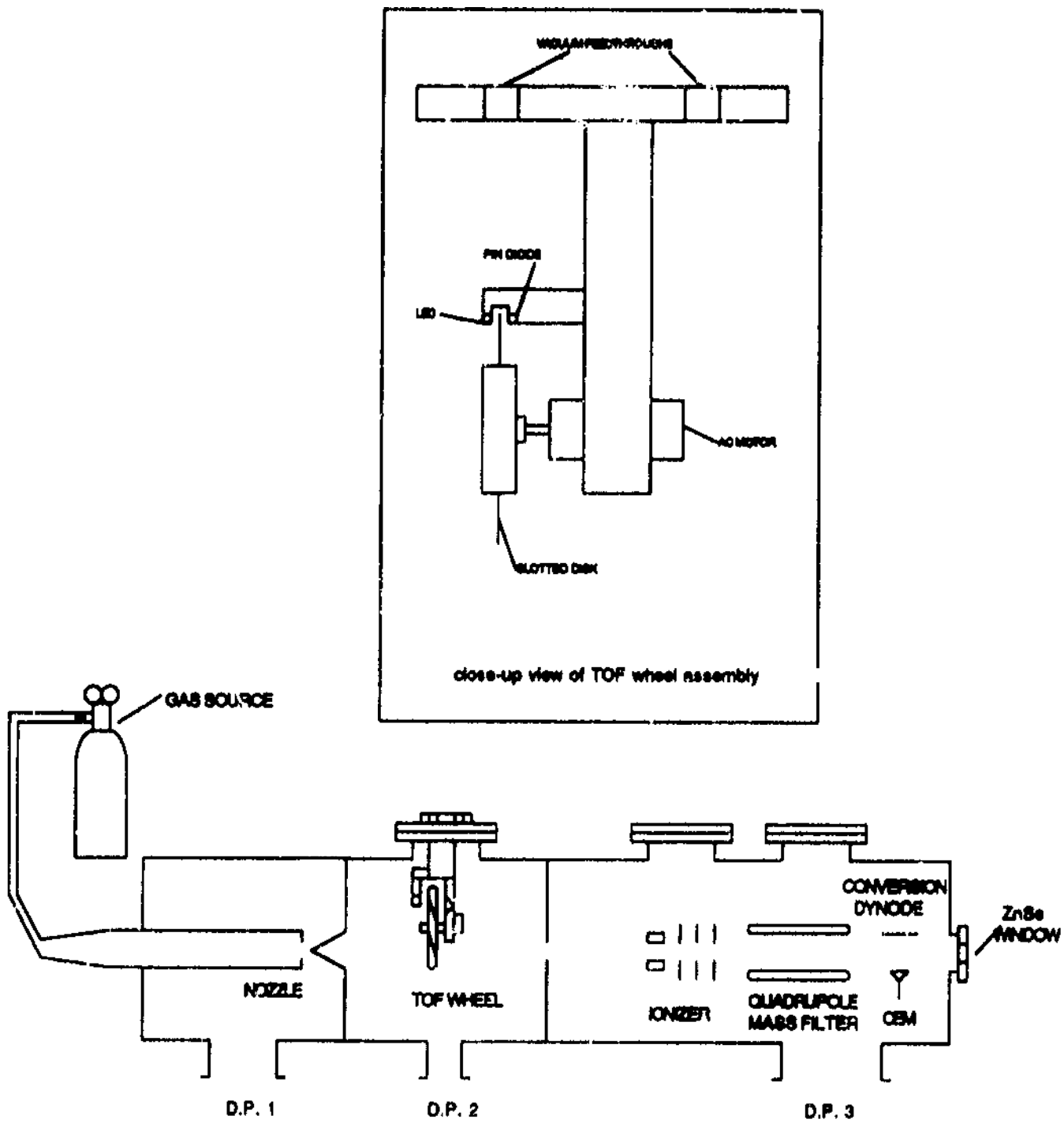

Figure 1. Ion-Beam apparatus in neutral configuration

Figure 2. Neutral beam apparatus.

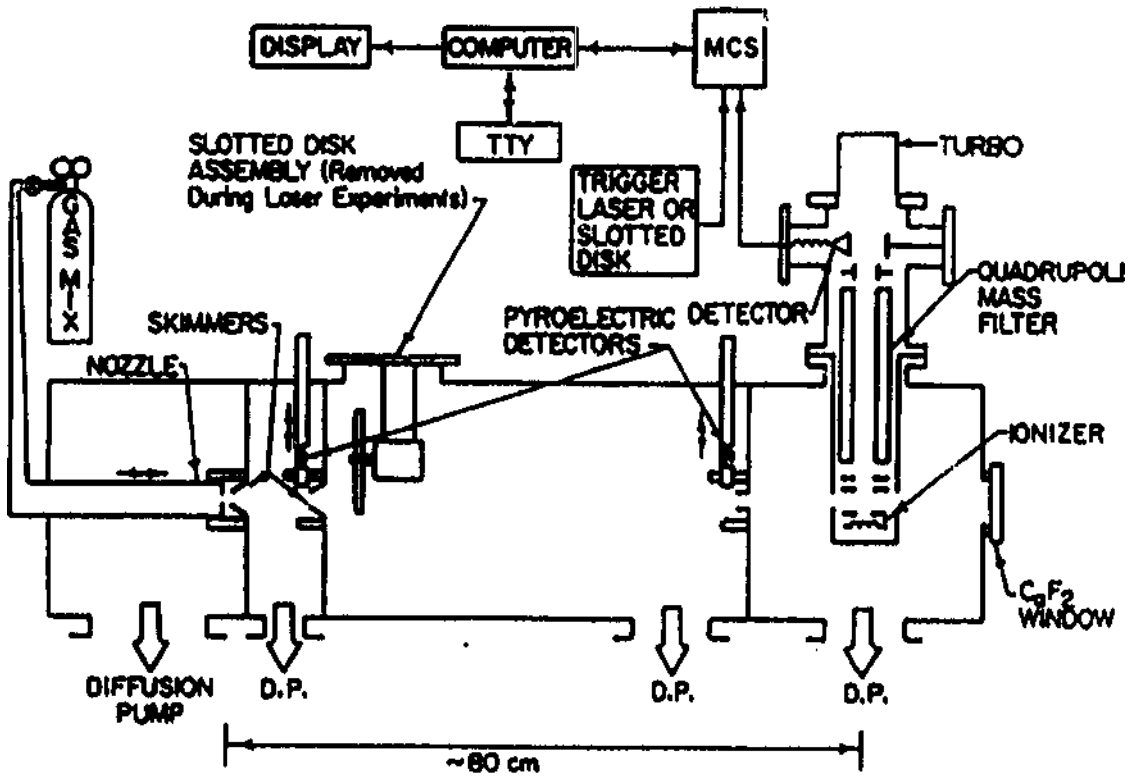
DISPLAY
COMPUTER
MCS
TTY
SLOTTED DISK ASSEMBLY (Removed During Laser Experiments)
TRIGGER LASER OR SLOTTED DISK
TURBO
GAS MIX
SKIMMERS
NOZZLE
PYROELECTRIC DETECTOR
DETECTORS
QUADRUPOLE MASS FILTER
IONIZER
C_9F_2 WINDOW
DIFFUSION PUMP
D.P.
D.P.
D.P.
~80 cm

RESULTS AND DISCUSSION

Tables 1 and 2 contain the temperatures obtained at several backing pressures and at different mass to charge ratios (m/e). The neutral clusters are ionized indiscriminately at the end of the flight path by electron bombardment. The cracking pattern is very complex and it is impossible to be absolutely sure of the contribution of different clusters at each observed mass peak. For the methanol data, the detected masses are due to positively charged clusters of the form $(MeOH)_xH^+$; water is found at masses corresponding to $(H_3O^+)(H_2O)_x$. The largest m/e values should be limited to the smallest range of cluster sizes. While the methanol dimer and each larger cluster could contribute to the peak at 33 amu, there are very few clusters formed that show up at 865 amu. The methanol 28-mer will be the principal precursor for the ion in the later case.

The most promising method for eliminating the effect of larger clusters in the neutral beam involves the use of a secondary beam to scatter the target beam, and the use of a rotating mass spectrometer detector.[9] Larger masses will be deflected less, causing the masses to separate. Detecting only those scattered clusters above a certain angle from the original beam axis excludes the unwanted higher order clusters.

The TOF apparatus requires recalibration for every set of ionization and electrostatic lens conditions; the settings used in this experiment are shown in appendix 1. A experimental equation for ion flight times at this ionization energy was determined by analysing the proportional speeds of the charged species produced

from the ionization of SF_6[9]. The nominal neutral flight length of the unionized clusters was obtained by comparing a experimentally obtained Ar beam flow velocity to the theoretical value under the same source conditions. Each set of data requires calculation of the correct delay parameters. A sample of these calculations is provided in appendix 2.

While comparisons of monatomic gases at varying pressures show a close relationship between backing pressure and terminal beam temperature (figure 3), the clusters of more complicated molecules behave less predictably. As can be seen in figure 4, only the largest mass follows the expected trend of more cooling at greater pressure differentials. Another theoretically forecast and previously observed result is the higher temperatures of larger clusters (see reference 4 and figure 5).

These experimental translational temperatures can also be applied to the research of solvated ions. The solvated ion complex is already charged, so no ionization is required for the quadrupole mass selection; this makes direct probing of specific clusters more precise. It is believed that in our apparatus, homogeneous clusters of solvent molecules are formed in the expansion stage, with carrier gas molecules cooling them through collisional energy transfer. After formation, the ion collides with the solvent and after some rearrangement the ion settles into a cluster followed by the release of excess energy by boiling off solvent molecules. In the study of cesium ion solvation by methanol, the detected masses are due to the complex formed after the evaporative loss of methanols during the transit time to the quadrupole.

The combination of the translational energy determined in our experiment plus the kinetic energy of the metal ion combine to give a lower limit to the total energy of the solvated ion. With this internal energy approximation, the number of molecules that must evaporate to "cool" the solvated ion to a temperature where it will remain stable for the time of the experiment can be calculated from theory.[10]

TABLE 1. TOF results for $(MeOH)_xH^+$ -- x = 7 to 27. The uncertainty listed is the intermediate reduced standard deviation of the fitted data from a Maxwellian velocity distribution.

X	Backing Pressure (Torr)	Temp. (°K) (+/-)
27	956.7	140 (11)
27	698.2	162 (23)
27	517.1	190 (17)
22	956.7	149 (12)
22	698.2	116 (8)
22	517.1	102 (10)
17	956.7	93 (9)
17	698.2	83 (26)
17	517.1	92 (5)
12	956.7	70 (8)
12	698.2	58 (4)
12	517.1	59 (5)
7	956.7	25 (4)
7	698.2	23 (4)
7	517.1	22 (8)

TABLE 2. TOF results for methanol clusters from neutral beam apparatus.

$(MeOH)_xH^+$ -- x = 1 to 11

N	Backing Pressure (Torr)	Temp. (°K)(+/-)
1	200	35.8 (4.9)
1	500	23.5 (2.2)
1	900	23.3 (3.5)
2	200	61.2 (7.1)
2	500	34.6 (2.9)
2	900	27.0 (3.0)
3	200	75.2 (11.3)
3	500	49.5 (6.0)
3	900	38.6 (4.5)
4	500	64.2 (8.8)
4	900	49.7 (6.3)
5	500	73.7 (13.1)
5	900	62.7 (9.3)
6	500	83.8 (15.0)
6	900	63. (10.9)
7	900	68.1 (9.3)
8	900	48.9 (12.7)
9	900	92.2 (14.3)
10	900	101.1 (18.7)
11	900	11.8 (21.8)

Figure 3. Rare Gas TOF Data.

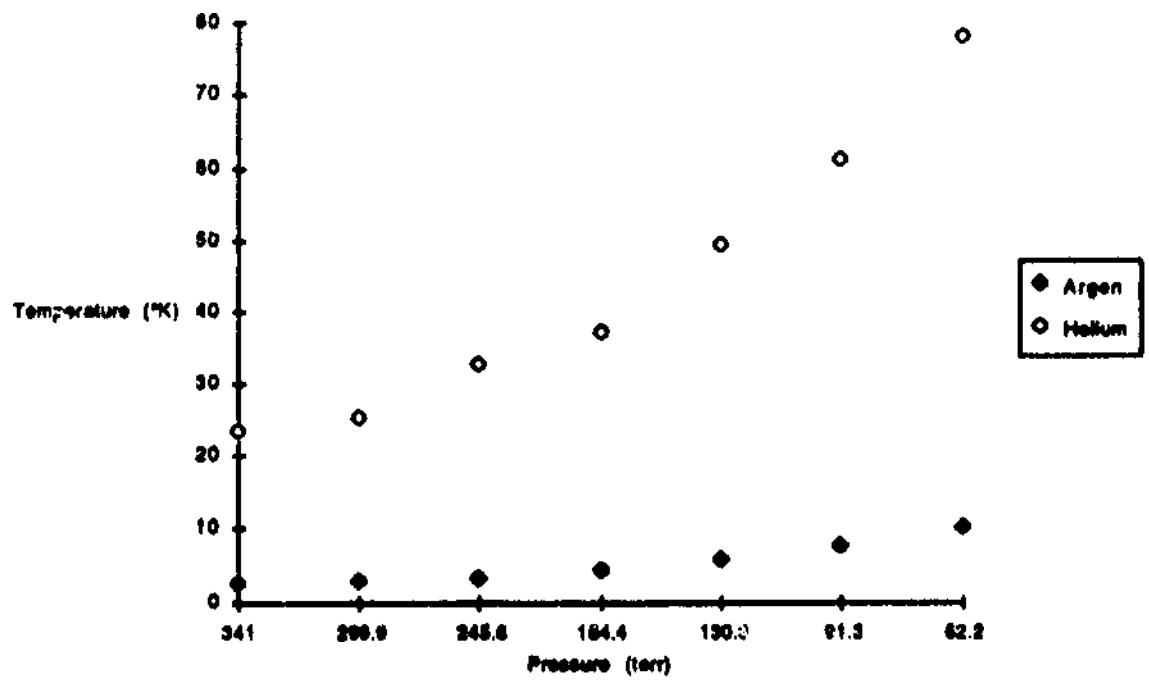
Temperature (°K)
0
10
20
30
40
50
60
70
80
341
Pressure (torr)
Argon
Helium

Figure 4. Methanol Temperature vs. Backing Pressure.

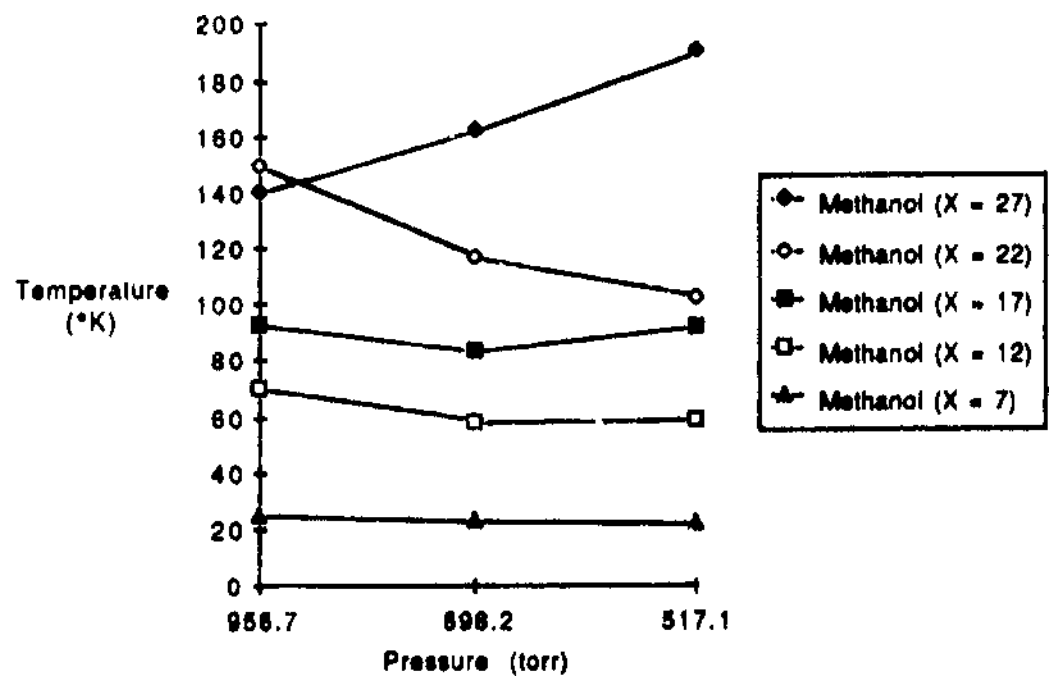
200
180
160
140
120
100
80
60
40
20
0
Temperature
(°K)
956.7
698.2
517.1
Pressure (torr)
Methanol (X = 27)
Methanol (X = 22)
Methanol (X = 17)
Methanol (X = 12)
Methanol (X = 7)

Figure 5. Methanol Temperature vs. Cluster Size.

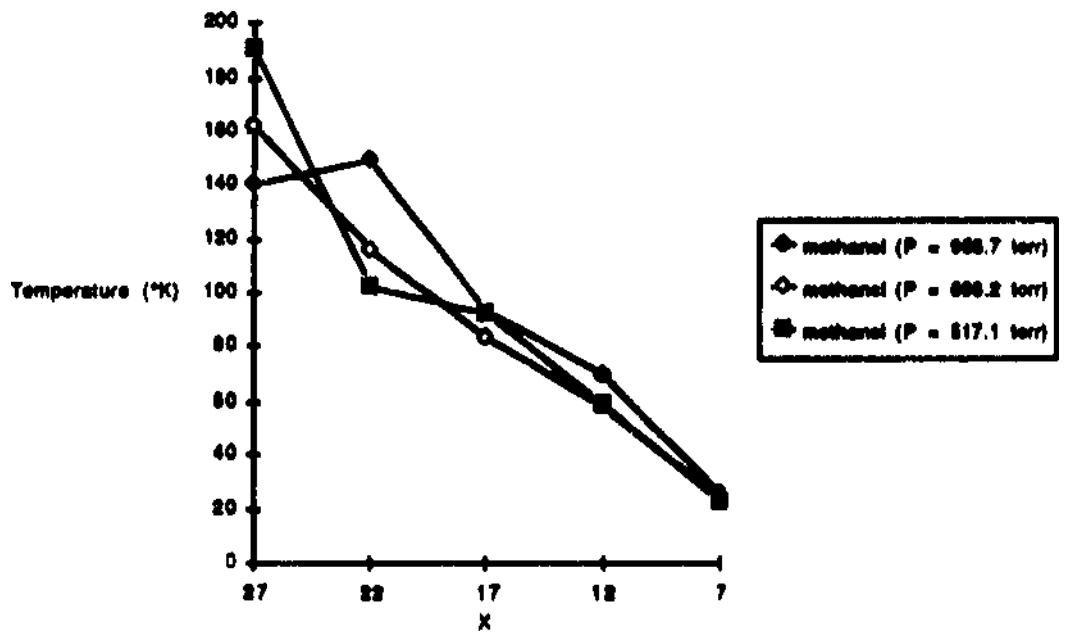
Temperature (°K)
200
180
160
140
120
100
80
60
40
20
0
27
22
17
12
7
X
methanol (P = 517.1 torr)

APPENDIX 1

Typical ionizer, ion optics, and detector settings used for Ar, He, SF_6, H_2O, and MeOH TOF:

Ion-Beam Apparatus		Neutral-Beam Apparatus	
CEM	+ 2800 V	Emission Current	6.0 mA
Ion Plate	+ 29 V	Filament Bias	- 60.0 V
Extractor	+19 V	Ion Energy	16.0 V
Lens 1	- 205 V	Extractor	11. V
Lens 2	0 V	Lens 1	- 389 V
Lens 3	+ 26 V	Lens 2	- 393 V
Quad.	- 97 V	Lens 3	8 V
Filament Bias	- 60 V	Lens 4	- 44 V
Electron Current	16.5 mA	Exit Lens 1	- 70 V
		Exit Lens 2	- 1700 V
		Photomultiplier Tube	- 1900 V
		Threshold/Discriminator	10 mV
		Doorknob	- 40000 V

APPENDIX 2

Equation 1. is used to determine the total offset delay for the Kelvin.

$$t_{offset} = t_E - t_{ion} + t_D + t_W \qquad \text{(Eq. 1)}$$

t_E: the electronic offset given by the time between the leading edge of the trigger pulse at the MCS trigger input and the maximum of the photodiode signal.

t_{ion}: the ion flight time dependent on ion energy.

t_D: digital delay used during data collection to keep long flight times managable.

t_W: time delay resulting from the offset between the peak of the photodiode signal and when the wheel slit is centered on the detector slit.

An example of a Kelvin output file is shown in Appendix 3. The steps taken to calculate t_{offset} for this data are listed below.

t_E = 9.0 channels (1.0 microseconds per channel)

This is constant for a particular wheelspeed and is determined experimentally.

t_{ion} = 254.0 channels

This is calculated from the experimental formula obtained by taking the slope (C) of the line corresponding to the SF_6 electron impact fragments flight times versus their charge to mass ratios (see figure 6).

$$t_{ion} = C * \sqrt{mass} \quad \text{(Eq. 2)}$$

for mass = 896 amu, and C = 8.5

t_{ion} = 254.0

t_D = 600.0 channels

This is simply the electronic delay used during data collection.

t_W = 9.0 channels

This corrects for the delay between the time the LED signal is observed and the time that the beam is centered on the beam axis. The location of the peak when the wheel direction is forward is subtracted from the reverse peak value and then used to offset the peaks so that they overlap.

$$t_W \text{ (forw./rev.)} = (+/-)\ (F-R)/2 = (227 - 245)/2 = +/- 9.0$$

$$t_{offset} = t_E - t_{ion} + t_D + t_W = 9 - 254 + 600 +/- 9 = 364 \text{ and } 346$$

Figure 6. SF_6 ion flight time determination.

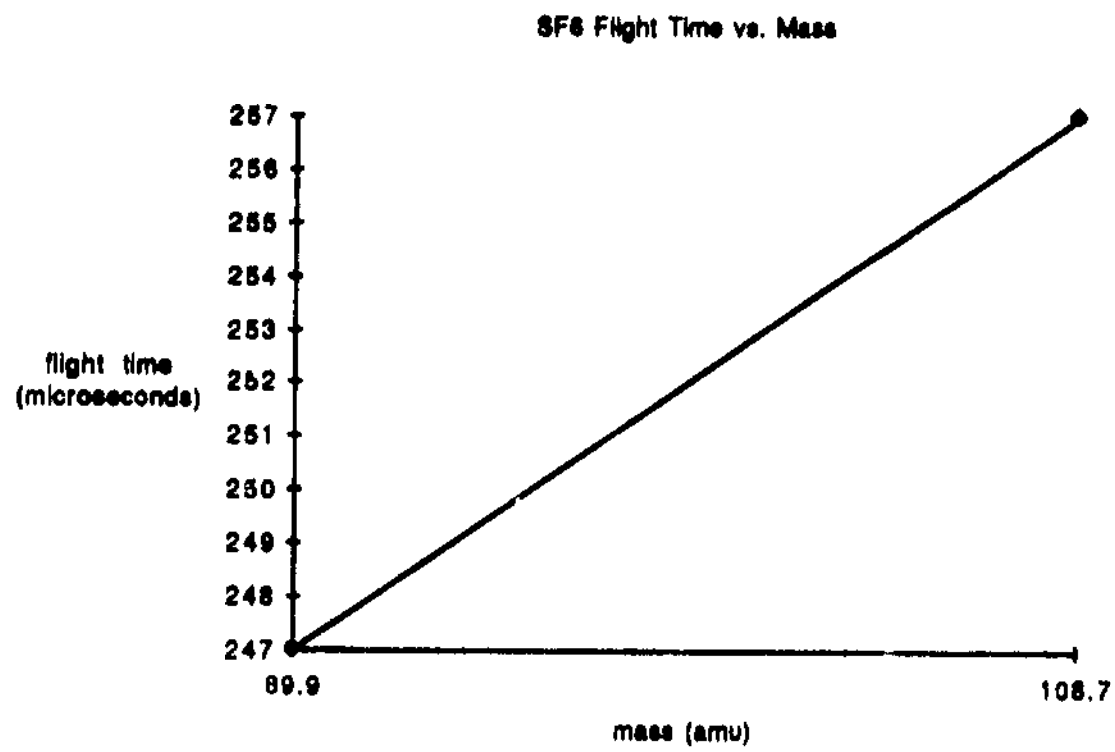
SF6 Flight Time vs. Mass
flight time
(microseconds)
257
256
255
254
253
252
251
250
249
248
247
89.9
108.7
mass (amu)

APPENDIX 3

Sample Kelvin Output File

METHANOL TOF 40 FORWARD

MASS =896.000
CHANNEL WIDTH = 1.0 MICROSECONDS; BEGINNING CHANNEL =134, ENDING CHANNEL =320; FLIGHT LENGTH =38.39 CM; IONIZER LENGTH = 1.00 CM.
OFFSET= 363.60 CHANNELS
WHEEL FREQ. =390. HZ; WHEEL DIAMETER = 5.1 CM; SLOT WIDTH = 0.79 MM; DETECTOR APERTURE =3.00 MM

INPUT DISTRIBUTION

134	11.6	135	13.0	136	13.3	137	14.7	138	14.7	139	14.6	140	14.9	141	15.1
142	14.9	143	16.7	144	17.6	145	18.7	146	19.7	147	21.0	148	23.1	149	23.7
150	25.0	151	25.6	152	28.7	153	31.3	154	31.4	155	32.0	156	34.6	157	36.6
158	39.3	159	44.1	160	48.9	161	52.4	162	54.3	163	59.1	164	62.4	165	65.0
166	64.4	167	66.3	168	69.7	169	79.4	170	83.6	171	89.1	172	100.1	173	107.3
174	113.7	175	121.1	176	121.6	177	128.4	178	133.4	179	139.1	180	144.7	181	151.0
182	154.6	183	164.3	184	171.0	185	178.0	186	183.1	187	191.6	188	196.1	189	203.9
190	211.4	191	222.0	192	234.7	193	240.6	194	251.4	195	262.6	196	274.3	197	285.7
198	294.3	199	302.7	200	312.4	201	311.9	202	318.6	203	330.7	204	338.6	205	348.4
206	355.3	207	362.3	208	376.4	209	391.1	210	395.0	211	402.0	212	407.4	213	407.6
214	413.1	215	412.9	216	410.6	217	413.3	218	419.9	219	421.1	220	427.6	221	428.0
222	435.6	223	440.9	224	450.1	225	447.6	226	452.4	227	452.7	228	452.1	229	450.7
230	447.7	231	439.7	232	441.6	233	435.6	234	434.0	235	436.0	236	436.9	237	434.3
238	432.6	239	420.9	240	421.0	241	414.9	242	408.3	243	400.7	244	393.6	245	388.9
246	392.0	247	380.6	248	375.7	249	373.3	250	362.3	251	357.0	252	355.6	253	345.1
254	341.7	255	341.1	256	335.0	257	328.1	258	320.9	259	311.9	260	305.3	261	295.9
262	284.7	263	279.6	264	281.6	265	278.9	266	273.7	267	269.7	268	265.7	269	256.1
270	245.3	271	238.0	272	230.1	273	222.6	274	217.1	275	211.9	276	209.9	277	209.3
278	201.9	279	192.9	280	190.1	281	184.0	282	180.3	283	179.0	284	173.4	285	170.1
286	170.3	287	163.0	288	158.4	289	154.7	290	149.9	291	142.6	292	137.1	293	131.6
294	129.3	295	124.7	296	116.9	297	112.9	298	110.4	299	107.7	300	103.7	301	99.1
302	95.3	303	92.3	304	87.3	305	86.6	306	84.1	307	81.4	308	78.3	309	76.3
310	75.0	311	74.1	312	70.0	313	69.6	314	67.4	315	66.0	316	65.9	317	65.3
318	61.7	319	59.3	320	55.7										

SHUTTER FUNCTION TRAPEZOID:

0.000731	0.002364	0.003998	0.005633
0.007267	0.008902	0.010537	0.012171
0.013806	0.015440	0.017075	0.018710
0.020292	0.020747	0.020747	0.020747
0.020747	0.020747	0.020747	0.020747
0.020747	0.020747	0.020747	0.020747
0.020747	0.020747	0.020747	0.020747
0.020747	0.020747	0.020747	0.020747
0.020747	0.020747	0.020747	0.020747
0.020747	0.020747	0.020747	0.020747
0.020747	0.020747	0.020747	0.020747
0.020747	0.020747	0.020747	0.020747
0.020292	0.018710	0.017075	0.015440
0.013806	0.012171	0.010537	0.008902
0.007267	0.005633	0.003998	0.002364

0.000731

INTERMEDIATE VALUES

STANDARD DEVIATION= 0.421E+00 DBETA= -0.4331E+00 DVZRO= -0.7408E-01

FINAL PARAMETER VALUES

BETA= 0.3680E+01 VZRO= 0.6402E+01 SPEED RATIO= 0.1228E+02 ALPHA= 0.5213E+00 ITERATIONS= 1 AVERAGE DEVIATION= 0.6
ESTIMATED ERROR IN LOCATION OF MINIUM ON SURFACE IN BETA AND VZRO= 0.3613E-01 0.2818E-02
ESTIMATED ERROR IN THE DERIVED PARAMETERS BETA AND VZRO= 0.3921E+00 0.3058E-01

TERMINAL BEAM TEMPERATURE= 147.4742 +/- 14.1987

C A L C U L A T E D D I S T R I B U T I O N

164	57.8	165	62.2	166	66.8	167	71.6	168	76.6	169	81.8	170	87.1	171	92.7
172	98.4	173	104.3	174	110.4	175	116.6	176	123.0	177	129.5	178	136.3	179	143.1
180	150.1	181	157.3	182	164.6	183	171.9	184	179.4	185	187.1	186	194.7	187	202.5
188	210.4	189	218.3	190	226.2	191	234.2	192	242.2	193	250.3	194	258.3	195	266.3
196	274.3	197	282.2	198	290.1	199	297.9	200	305.6	201	313.2	202	320.7	203	328.1
204	335.3	205	342.4	206	349.3	207	356.1	208	362.6	209	368.9	210	375.0	211	380.9
212	386.6	213	391.9	214	397.1	215	401.9	216	406.5	217	410.8	218	414.8	219	418.6
220	421.8	221	424.9	222	427.7	223	430.1	224	432.2	225	433.9	226	435.4	227	436.5
228	437.2	229	437.7	230	437.8	231	437.6	232	437.0	233	436.1	234	434.9	235	433.4
236	431.6	237	429.5	238	427.1	239	424.4	240	421.4	241	418.1	242	414.6	243	410.8
244	406.8	245	402.5	246	398.0	247	393.3	248	388.3	249	383.2	250	377.9	251	372.4
252	366.7	253	360.9	254	355.0	255	348.9	256	342.7	257	336.4	258	330.0	259	323.5
260	316.9	261	310.3	262	303.6	263	296.9	264	290.1	265	283.3	266	276.5	267	269.7
268	262.9	269	256.1	270	249.3	271	242.6	272	235.8	273	229.2	274	222.6	275	216.0
276	209.5	277	203.1	278	196.7	279	190.4	280	184.3	281	178.2	282	172.2	283	166.2
284	160.4	285	154.7	286	149.1	287	143.6	288	138.3	289	133.0	290	127.9		

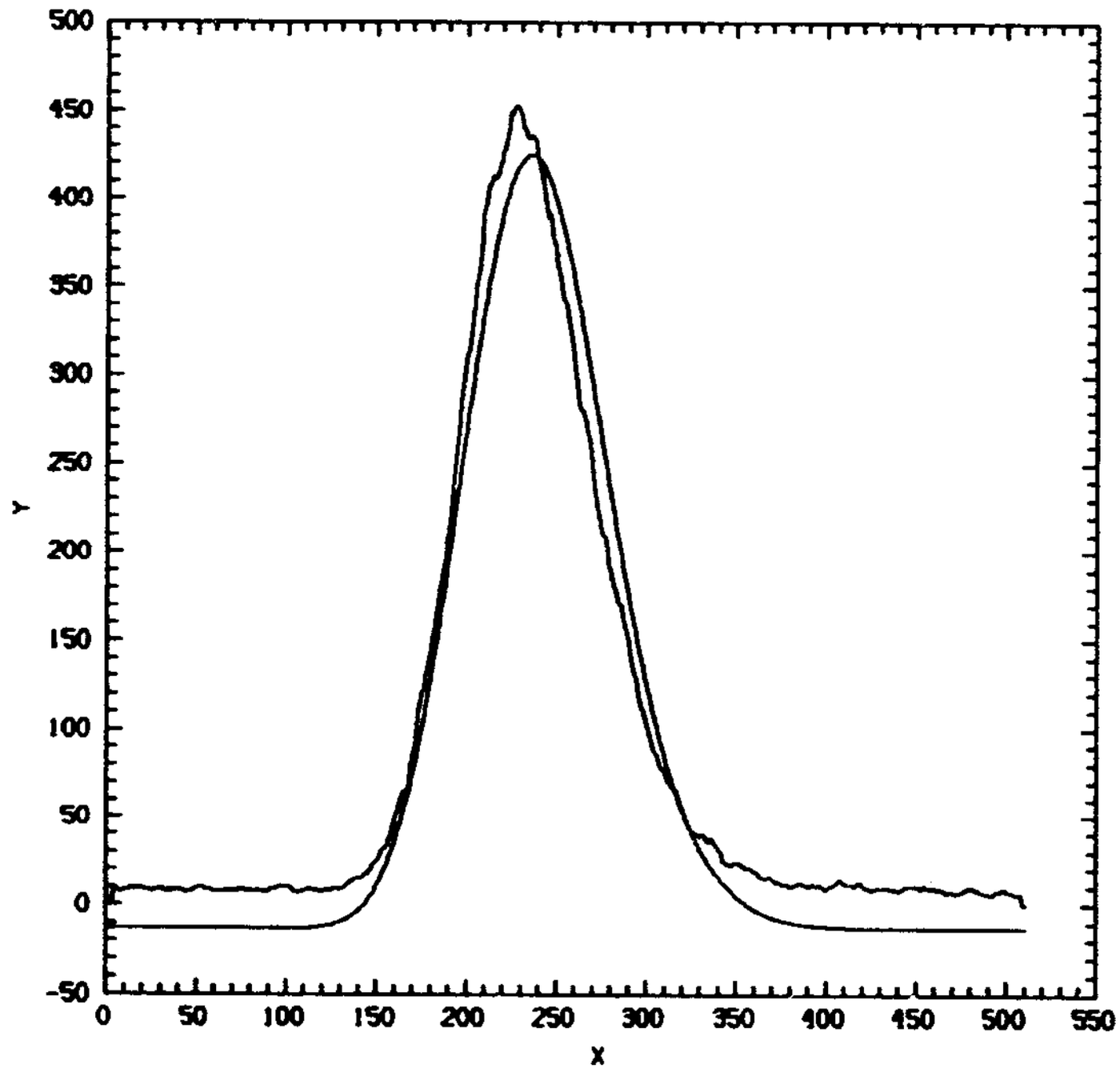
500
450
400
350
300
250
200
150
100
50
0
-50
Y
0
50
100
150
200
250
300
350
400
450
500
550
X

METHANOL TOF 40 REVERSE

MASS =896.000
CHANNEL WIDTH = 1.0 MICROSECONDS; BEGINNING CHANNEL =151, ENDING CHANNEL =339; FLIGHT LENGTH =38.39 CM; IONIZER LENGTH = 1.00 CM.
OFFSET= 345.80 CHANNELS
WHEEL FREQ. =390. HZ; WHEEL DIAMETER = 5.1 CM; SLOT WIDTH = 0.79 MM; DETECTOR APERTURE =3.00 MM

I N P U T D I S T R I B U T I O N

151	12.6	152	13.1	153	15.7	154	16.9	155	16.6	156	16.6	157	16.7	158	17.6
159	19.6	160	20.0	161	19.6	162	21.0	163	22.4	164	24.3	165	24.3	166	25.7
167	26.0	168	28.6	169	29.1	170	30.3	171	31.7	172	33.6	173	33.4	174	34.6
175	37.4	176	40.9	177	44.6	178	47.4	179	52.0	180	56.4	181	64.9	182	68.0
183	69.9	184	74.4	185	77.0	186	80.0	187	82.6	188	81.7	189	83.1	190	89.3
191	90.9	192	96.9	193	101.1	194	109.0	195	118.4	196	129.0	197	135.3	198	144.0
199	146.6	200	153.3	201	160.0	202	158.1	203	173.9	204	178.4	205	169.4	206	201.0
207	208.1	208	214.1	209	220.0	210	229.1	211	238.7	212	244.9	213	255.3	214	267.7
215	277.9	216	288.1	217	292.0	218	302.7	219	308.6	220	308.7	221	313.1	222	318.3
223	327.9	224	339.0	225	347.1	226	353.7	227	367.3	228	369.1	229	379.0	230	381.3
231	387.4	232	392.7	233	399.1	234	406.0	235	409.0	236	409.9	237	413.9	238	411.9
239	407.6	240	406.7	241	409.6	242	425.6	243	429.4	244	425.9	245	429.6	246	435.4
247	429.1	248	422.9	249	412.1	250	405.1	251	406.7	252	397.1	253	396.0	254	397.9
255	394.3	256	386.6	257	384.3	258	380.6	259	379.1	260	368.4	261	362.1	262	353.9
263	358.7	264	355.7	265	349.1	266	342.7	267	341.0	268	331.6	269	324.9	270	308.9
271	297.1	272	295.3	273	284.9	274	281.1	275	275.9	276	270.7	277	266.3	278	259.6
279	245.9	280	240.6	281	222.9	282	214.6	283	208.0	284	201.7	285	193.0	286	182.9
287	179.1	288	177.7	289	175.1	290	158.0	291	161.0	292	154.1	293	149.0	294	143.7
295	136.0	296	128.6	297	122.3	298	117.6	299	118.4	300	114.7	301	108.0	302	105.1
303	99.0	304	96.1	305	92.4	306	89.3	307	83.4	308	82.7	309	79.9	310	78.0
311	75.7	312	72.3	313	70.0	314	68.1	315	64.6	316	62.0	[illegible]	60.0	318	54.6
319	53.1	320	49.3	321	46.4	322	43.7	323	42.0	324	39.1	325	40.4	326	38.1
327	37.4	328	36.1	329	34.6	330	33.4	331	33.1	332	30.1	333	29.3	334	28.6
335	28.6	336	27.9	337	28.6	338	29.0	339	28.3						

SHUTTER FUNCTION TRAPEZOID:

0.000731	0.002364	0.003998	0.005633
0.007267	0.008902	0.010537	0.012171
0.013806	0.015440	0.017075	0.018710
0.020292	0.020747	0.020747	0.020747
0.020747	0.020747	0.020747	0.020747
0.020747	0.020747	0.020747	0.020747
0.020747	0.020747	0.020747	0.020747
0.020747	0.020747	0.020747	0.020747
0.020747	0.020747	0.020747	0.020747
0.020747	0.020747	0.020747	0.020747
0.020747	0.020747	0.020747	0.020747
0.020747	0.020747	0.020747	0.020747
0.020292	0.018710	0.017075	0.015440
0.013806	0.012171	0.010537	0.008902
0.007267	0.005633	0.003998	0.002364

0.000731

INTERMEDIATE VALUES

STANDARD DEVIATION= 0.563E+00 DBETA= 0.5457E-02 DVZRO= -0.1042E-01

FINAL PARAMETER VALUES

BETA= 0.3850E+01 VZRO= 0.6453E+01 SPEED RATIO= 0.1266E+02 ALPHA= 0.5096E+00 ITERATIONS= 1 AVERAGE DEVIATION= 0.7
ESTIMATED ERROR IN LOCATION OF MINIUM ON SURFACE IN BETA AND VZRO= 0.2580E-01 0.2467E-02
ESTIMATED ERROR IN THE DERIVED PARAMETERS BETA AND VZRO= 0.3405E+00 0.3257E-01

TERMINAL BEAM TEMPERATURE= 140.9632 +/- 11.4534

C A L C U L A T E D D I S T R I B U T I O N

181	44.0	182	48.7	183	53.7	184	58.7	185	64.0	186	69.5	187	75.1	188	81.0
189	87.0	190	93.2	191	99.5	192	106.0	193	112.7	194	119.5	195	126.5	196	133.6
197	140.9	198	148.3	199	155.7	200	163.3	201	171.0	202	178.8	203	186.6	204	194.5
205	202.5	206	210.5	207	218.5	208	226.5	209	234.5	210	242.5	211	250.4	212	258.3
213	266.2	214	273.9	215	281.6	216	289.1	217	296.6	218	303.9	219	311.0	220	318.0
221	324.8	222	331.4	223	337.8	224	344.0	225	350.0	226	355.7	227	361.1	228	366.3
229	371.2	230	375.8	231	380.2	232	384.2	233	387.9	234	391.3	235	394.4	236	397.1
237	359.6	238	401.6	239	403.4	240	404.8	241	405.8	242	406.6	243	406.9	244	407.0
245	406.6	246	406.0	247	405.0	248	403.7	249	402.1	250	400.2	251	397.9	252	395.3
253	392.5	254	389.3	255	385.9	256	382.2	257	378.2	258	374.0	259	369.6	260	364.9
261	360.0	262	354.9	263	349.6	264	344.1	265	338.4	266	332.6	267	326.6	268	320.5
269	314.3	270	308.0	271	301.5	272	295.0	273	288.3	274	281.7	275	274.9	276	268.1
277	261.3	278	254.5	279	247.6	280	240.8	281	233.9	282	227.1	283	220.2	284	213.5
285	206.7	286	200.0	287	193.4	288	186.8	289	180.3	290	173.9	291	167.5	292	161.3
293	155.1	294	149.1	295	143.1	296	137.2	297	131.5	298	125.8	299	120.3	300	114.9
301	109.6	302	104.4	303	99.3	304	94.4	305	89.6	306	84.9	307	80.3	308	75.9
309	71.6														

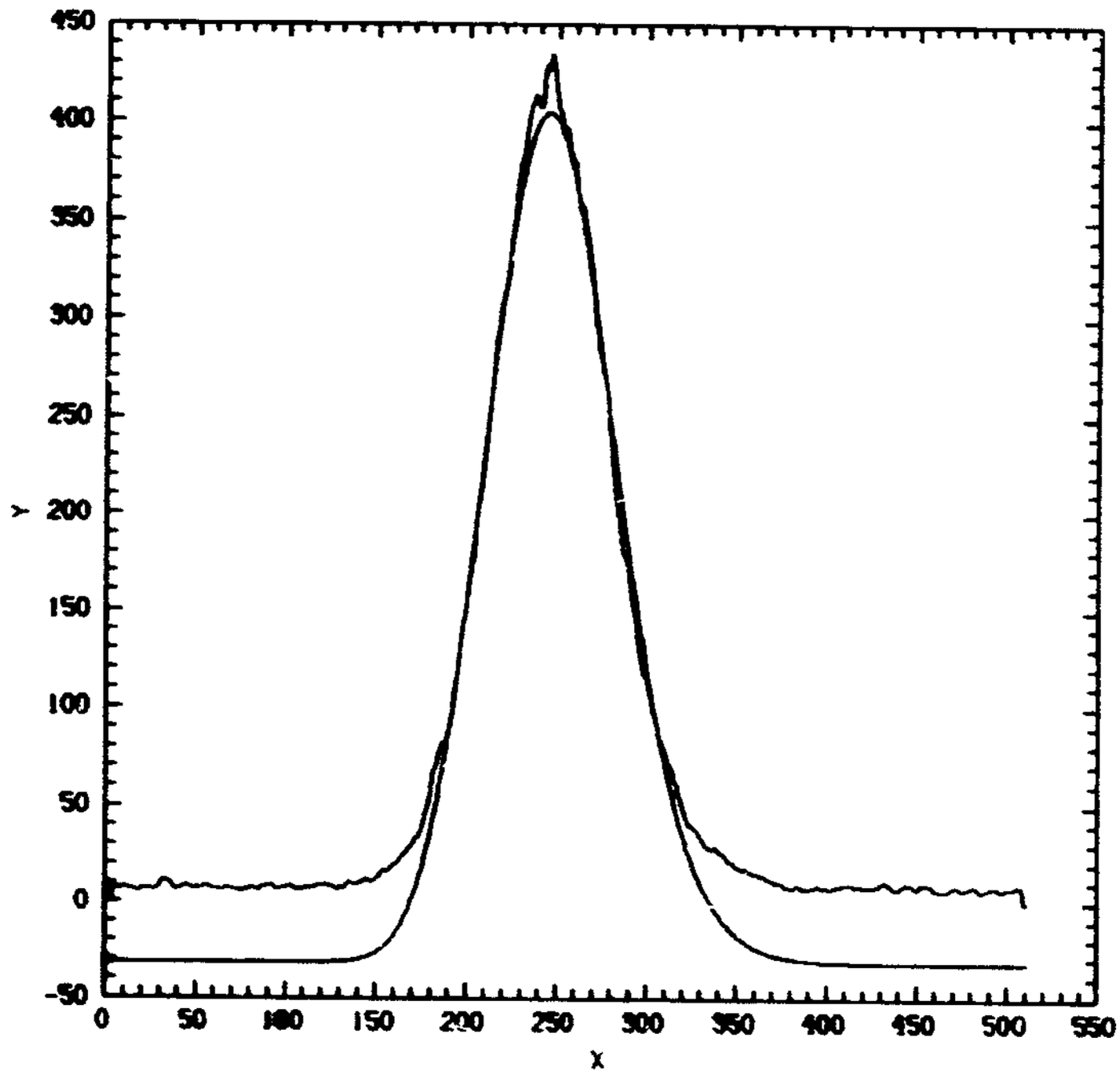
450
400
350
300
250
200
150
100
50
0
-50
Y
0
50
100
150
200
250
300
350
400
450
500
550
X

REFERENCES AND NOTES

[1]W.L. Taylor, R.W. York, and P.T. Pickett, in "Rarefied Gas Dynamics," ed. S.S. Fisher, Progress in Astronautics and Aeronautics (American Institute of Aeronautics and Astronautics, New York, 1980).

[2]J.B. Anderson, R.P. Andres, and J.B. Fenn, "Supersonic Nozzle Beams," Advances in Chemical Physics 10, (Academic, New York, 1976).

[3]H. Haberland, U. Buck, and M. Tolle, Rev. Sci. Instrum. 56, 9 (1985).

[4]D. Dreyfuss, H.Y. Wachman, J. Chem. Phys. 76, (1982).

[5]D.W. Michael, J.M. Lisy, J. Chem. Phys. 85, 56 (1986).

[6]M. Vernon, "Kelvin Rare Gas Time of Flight Program," (National Technical Information Service, 1981).

[7]W.L. Liu, "Production and Vibrational Predissociation of Solvated Alkali Ions," PhD. Thesis, University of Illinois, 1989.

[8]U. Buck, et. al., J. Phys. Chem. 92, 20 (1988).

[9]Appendix 2 contains a more detailed description of this procedure.

[10]The dissociation occurs in the quadrupole region. Therefore, the minimum lifetime needed for the complex to reach the detector is about 25 microseconds, which is the ion flight-time through the quadrupole.